nature physics

ARTICLES

PUBLISHED ONLINE: 7 SEPTEMBER 2015 | DOI: 10.1038/NPHYS3456

Nematicity and quantum paramagnetism in FeSe

Fa Wang[1,2], Steven A. Kivelson[3] and Dung-Hai Lee[4,5]*

In common with other iron-based high-temperature superconductors, FeSe exhibits a transition to a 'nematic' phase below 90 K in which the crystal rotation symmetry is spontaneously broken. However, the absence of strong low-frequency magnetic fluctuations near or above the transition has been interpreted as implying the primacy of orbital ordering. In contrast, we establish that quantum fluctuations of spin-1 local moments with strongly frustrated exchange interactions can lead to a nematic quantum paramagnetic phase consistent with the observations in FeSe. We show that this phase is a fundamental expression of the existence of a Berry's phase associated with the topological defects of a Néel antiferromagnet, in a manner analogous to that which gives rise to valence bond crystal order for spin-1/2 systems. We present an exactly solvable model realizing the nematic quantum paramagnetic phase, discuss its relation with the spin-1 J_1–J_2 model, and construct a field theory of the Landau-forbidden transition between the Néel state and this nematic quantum paramagnet.

Insulating quantum paramagnets (PM) are magnetic systems with only short-range antiferromagnetic (AF) correlations even at zero temperature. Examples of quantum paramagnetic states include valence bond solids, symmetry-protected topological states, and spin liquids. Interest in quantum paramagnets was greatly intensified following the proposal[1] (since shown to be incorrect) that the parent insulator of the cuprate high-temperature superconductors (HTSC) might be a spin liquid. Because of the proposed relevance to the cuprates, special attention has been paid to square lattice $S=1/2$ systems, and in particular to the J_1–J_2 Heisenberg model,

$$H = J_1 \sum_{\langle ij \rangle} \mathbf{S}_i \cdot \mathbf{S}_j + J_2 \sum_{\langle\langle jk \rangle\rangle} \mathbf{S}_j \cdot \mathbf{S}_k \qquad (1)$$

where $\langle ij \rangle$ and $\langle\langle jk \rangle\rangle$ denote nearest-neighbour (NN) and second neighbour pairs of sites and J_1, J_2 are the associated coupling constants. Numerical studies have shown[2–4] that the ground state of equation (1) has Néel AF order for $0 \leq J_2/J_1 \lesssim 0.4$ and stripe AF order (see Fig. 1a,b) for $0.6 \lesssim J_2/J_1$. Both these phases have gapless $S=1$ (spin wave) excitations. For $0.4 \lesssim J_2/J_1 \lesssim 0.6$ the ground state seems to have no magnetic order. However, there remain important unresolved issues concerning the precise character of this phase or phases; at least for $0.5 \lesssim J_2/J_1 \lesssim 0.6$ there is fairly compelling evidence of translation-symmetry-breaking valence band solid order with an energy gap for spin-1 excitations.

The curious fact that on restoring the spin rotation symmetry the breaking of spatial translation symmetry follows, rests on a uniquely quantum mechanical effect associated with the Berry's phase of the monopole events[5,6]. A monopole (anti-monopole) is a spacetime event (see Fig. 2a) across which the 'skyrmion number' (see the caption of Fig. 2) changes by $+1(-1)$. The proliferation of monopoles randomizes the Néel order parameter, hence causing the system to become a PM. In ref. 5, it was argued that monopole events contribute to the path integral with a phase factor that depends on the monopole's spatial location (see Fig. 2b,c).

Spin models based on local moments, such as the J_1–J_2 model, have found renewed applications in the young field of iron-based superconductivity. The iron-based HTSCs have layers of Fe^{2+} ions which form a square lattice at high temperatures. Many experimental and theoretical studies have concluded that, with the possible exception of heavily phosphorus-doped members of the 122 family, the electronic correlations in the iron-based materials, in particular in the iron chalcogenides, are strong[7–9]. Moreover, relatively large local magnetic moments in many of these materials have been inferred[10]. For FeSe the itinerant electrons give rise only to tiny Fermi pockets[11–14]. Thus, it is plausible that the magnetism of FeSe can be addressed using a spin model as a starting point.

For many iron-based materials, depending on the doping level, there is 'stripe' AF order at low temperatures (see Fig. 1a,b). Owing to the breaking of crystal rotation symmetry the stripe order is accompanied by a tetragonal to orthorhombic lattice distortion. In some cases—for example, in electron-doped Ba-122 materials—the lattice distortion can exist without stripe order (see Fig. 3a). In ref. 15 it was shown that the distortion is driven by electronic nematicity rather than a lattice (phonon) instability. It has been argued that such nematicity reflects an underlying stripe ordering tendency, and the reason it can exist without the magnetic order is because thermal fluctuations of the continuously varying spin orientation are more severe than those of the discrete nematic director[16–18].

A potential problem with this perspective is the thermal evolution observed in FeSe crystals, in which nematicity onsets at $T_{\rm nem} \sim 90$ K, but there is no magnetic ordering down to the lowest measured temperatures, suggesting the possibility of a zero-temperature nematic quantum PM phase (Fig. 3b). This fact, coupled with the absence of any observed enhancement of the low-frequency magnetic fluctuations at $T_{\rm nem}$ (refs 19,20), has led many to concluded that the nematicity in FeSe is driven by orbital ordering.

Certainly, it is clear that within a local moment picture the lack of magnetic order implies that the spin–spin interactions must be highly frustrated; this is true regardless of what causes the nematic ordering. Thus in the following we ask, 'Can frustrated spin interactions alone drive a nematic quantum PM state?'

We consider models in which each Fe^{2+} possesses a localized spin 1 (for example, the $S=1$ version of the model in equation (1)).

[1]International Center for Quantum Materials, School of Physics, Peking University, Beijing 100871, China. [2]Collaborative Innovation Center of Quantum Matter, Beijing 100871, China. [3]Department of Physics, Stanford University, Stanford, California 94305, USA. [4]Department of Physics, University of California, Berkeley, California 94720, USA. [5]Materials Sciences Division, Lawrence Berkeley National Laboratory, Berkeley, California 94720, USA. *e-mail: dunghai@berkeley.edu

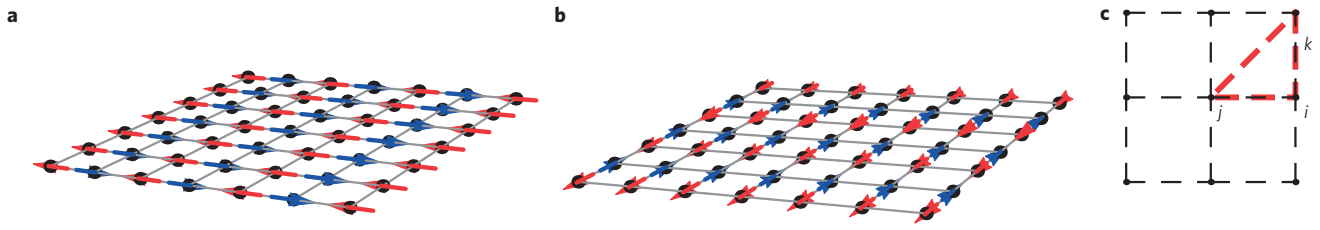

Figure 1 | The stripe AF and the interactions in H_K. a,b, Two degenerate versions of a stripe AF ground state corresponding to the two possible directions of the ordering vector, where the arrows schematically represent the ordered magnetic moments on the Fe sites. **c**, Three-site interaction corresponding to each individual projection operator from equation (2).

Given the strength of Hund's coupling and the crystal-field splittings, $S=1$ is a reasonable possibility for the spin of Fe^{2+} ions. However, it is important to keep in mind that FeSe is not an insulator, and such localized models neglect the effects of itinerant carriers. We shall return to this point later.

First we demonstrate the existence of a nematic quantum PM phase in an exactly solvable Hamiltonian. Consider a square lattice of $S=1$ spins interacting via the short-range, spin rotationally invariant Hamiltonian

$$H_K = K \sum_{\langle ijk \rangle} P_3(\mathbf{S}_i + \mathbf{S}_j + \mathbf{S}_k) \qquad (2)$$

where $K>0$ and $\sum_{\langle ijk\rangle}$ sums over all elementary triangles of sites (see Fig. 1c), and where $\overline{ji}$ and $\overline{ik}$ are NN bonds and $\overline{jk}$ is a next-NN bond. Here $P_3(\mathbf{S}) = (1/720)S^2(S^2-2)(S^2-6)$ is the projection operator onto $S=3$. We note that because it involves spin-1 operators, equation (2) possesses a global spin SO(3) (rather than SU(2)) symmetry. In addition it possesses all crystalline symmetries of the square lattice (that is, translation and point group symmetries). Moreover, there are two degenerate ground states which can be constructed exactly as follows: any closed loop $\mathcal{C}_{i_1,\ldots,i_n}$ on the lattice can be thought of as a spin-1 chain. The well-known AKLT (Affleck–Kennedy–Lieb–Tasaki) state[21] of such chains can be written as the matrix product state $|\mathcal{C}_{i_1,\ldots,i_n}\rangle = \sum_{m_{i_1}=-1}^{1} \cdots \sum_{m_{i_n}=-1}^{1} \mathrm{Tr}[A(m_{i_1}) \ldots A(m_{i_n})]|m_{i_1},\ldots,m_{i_n}\rangle$, where $m_{i_k}=-1,0,1$ is the S_z quantum number of the spin on site i_k, and the matrices $A(m)$ are $A(\pm1)=(\mp\sigma_x+i\sigma_y)/2\sqrt{2}, A(0)=\sigma_z/2$, with $\sigma_{x,y,z}$ being the Pauli matrices. We identify the two adjacent sites i_k and i_{k+1} in an AKLT loop as an 'AKLT-entangled pair', and graphically represent it by a blue bond connecting i_k and i_{k+1} in Fig. 4. The two ground states of H_K are constructed as the direct product of AKLT-loop states on all the loops made by connecting NN sites in the x direction, $|\mathrm{X}\rangle = \prod_{y=1}^{N} |\mathcal{C}_{(1,y),(2,y),\ldots,(N,y)}\rangle$, or in the y direction, $|\mathrm{Y}\rangle = \prod_{x=1}^{N} |\mathcal{C}_{(x,1),(x,2),\ldots,(x,N)}\rangle$, where (x,y) with $x,y=1,\ldots,N$ labels the sites of a $N\times N$ square lattice. The graphical representations of $|\mathrm{X}\rangle$ and $|\mathrm{Y}\rangle$ are shown in Fig. 4. Because the maximum total spin of an AKLT-entangled pair is $S=1$ (ref. 21), it follows that the maximum spin component of a triplet of spins $\langle ijk\rangle$ containing at least one AKLT-entangled pair is $S=2$. From this it follows trivially that H_K annihilates $|\mathrm{X}\rangle$ and $|\mathrm{Y}\rangle$; moreover, as H_K is positive semidefinite, this proves that they are ground states.

It is only slightly more difficult to see that any other state constructed as a direct product of AKLT-loop states has positive energy: as each site can be AKLT-entangled with at most two other sites, and as there are four elementary triangles per site, in any zero-energy state exactly two of the sites must be AKLT-entangled, and each entangled pair must form an edge of four distinct elementary triangles. The two states $|\mathrm{X}\rangle$ and $|\mathrm{Y}\rangle$ are the only ones that satisfy this constraint. For instance, if the blue bonds in Fig. 4 make a turn, an elementary triangle with its vertex at the corner of the turn will not contain any AKLT-entangled pair. Although we do not have a general proof that no more complex ground states exist, explicit finite cluster diagonalization (up to system size 4×4) suggests that there are none.

From the known properties of AKLT states[21,22], it follows immediately that $|\mathrm{X}\rangle$ and $|\mathrm{Y}\rangle$ are gapped PM states with exponentially falling spin–spin correlations which break crystal rotation symmetry: $G_X(\mathbf{R}_{ij}) \equiv \langle \mathrm{X}|\mathbf{S}_i \cdot \mathbf{S}_j|\mathrm{X}\rangle = 9\cos(\mathbf{R}_{ij}\cdot\mathbf{Q}_N)\delta(\mathbf{R}_{ij}\cdot\hat{y})e^{-|\mathbf{R}_{ij}\cdot\hat{x}|/\xi_0}$ with $\mathbf{Q}_N = \pi(\hat{x}+\hat{y})$ and $\xi_0 = 1/\ln(3)$ in units in which the lattice constant is 1. The gap implies that the nematic PM phase is perturbatively stable. However, the asymptotic form of G is non-generic—this reflects the fact that H_K lies on a 'disorder line[23]' where, although there is no associated thermodynamic non-analyticity, the oscillatory character of the short-range order changes.

Turning to less 'reverse engineered' models, we discuss the very interesting numerical (density matrix renormalization group) study by Jiang *et al.*[24] of the spin-1 version of the J_1–J_2 model in equation (1). They found that as a function of J_2/J_1 there is an intermediate paramagnetic phase (characterized by gapped $S=1$ excitations) between the Néel and stripe-ordered phases (see Fig. 3c). Moreover the Néel and stripe order parameters vanish continuously as J_2/J_1 approaches the respective critical values from the magnetically ordered side (see Fig. 4 of ref. 24). In the Supplementary Information we perform exact diagonalization on small lattices and demonstrate the adiabatic connectivity of the ground-state phases of H_K (equation (2)) and the J_1–J_2 model when J_2/J_1 falls within the PM regime. Furthermore, we compare the excitations in different spin and momentum sectors.

To obtain an analytic understanding of the nematic quantum PM phase, we consider a field theory description valid in the neighbourhood of a continuous or weakly first-order quantum phase transition from the Néel phase to a nematic PM phase. Because the unbroken symmetries of the Néel and nematic PM phases do not have a subgroup relationship, classical Landau theory would imply that such a continuous phase transition is forbidden. However, as pointed out in ref. 25, when the topological defects of one order carry the quantum number of the other order a continuous transition becomes possible.

According to ref. 5, in the path integral describing the quantum fluctuations of the $S=1$ Néel antiferromagnet in 2D, the weight associated with each field configuration is determined by the usual nonlinear sigma model (analogous to the first term in equation (3)), but there is also an additional Berry's phase factor. For a 'charge' q_m monopole (which causes the skyrmion number to jump by q_m) centred on plaquette $\boldsymbol{\mathcal{R}}$ (which designates a point on the dual lattice) this phase factor (up to a global 'gauge' ambiguity) is $\eta_{\boldsymbol{\mathcal{R}}} = e^{iq_m(\mathbf{Q}_N\cdot\boldsymbol{\mathcal{R}})}$ (see Fig. 2c). Rotation by 90° about a lattice site transforms $\eta_{\boldsymbol{\mathcal{R}}} \to -\eta_{\boldsymbol{\mathcal{R}}}$ but keeps q_m invariant. So long as this symmetry is preserved, the Feynman amplitude of any field configuration with an odd q_m cancels that associated with the configuration rotated by 90°. As a result, odd q_m monopoles cannot proliferate, although even q_m monopoles can. Consequently, states can be classified by a conserved skyrmion number parity $(-1)^{q_s}$. It turns out that the two-fold degeneracy associated with opposite skyrmion parity

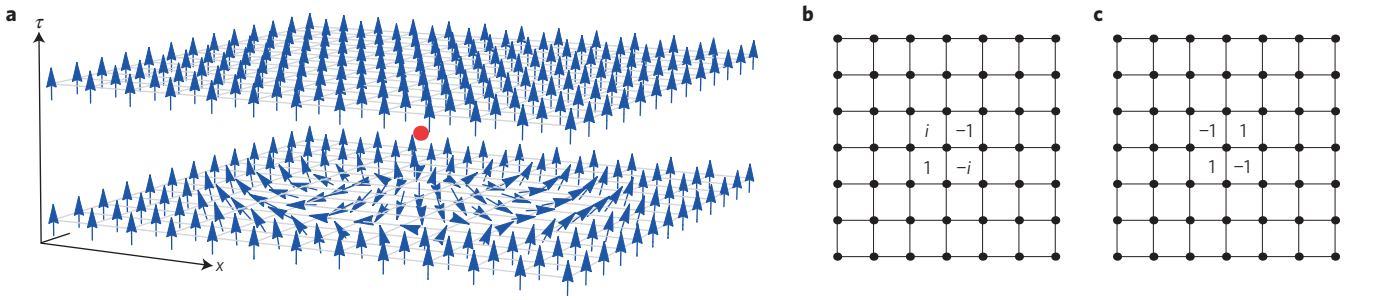

Figure 2 | The monopole phase factors. A monopole is a singular configuration of the Néel order parameter whose direction is depicted by an unit vector $\hat{n}$ at each point in space and time. The Néel order parameter configurations before and after a monopole event differ topologically—the skyrmion number changes by one. To understand the skyrmion number imagine assigning an unit vector to each point of a two-dimensional space subject to periodic boundary conditions. Such an assignment is a 'map' from a torus to the unit sphere S^2. These maps can be grouped into topological classes, where only maps within the same class can be smoothly deformed into one another. An integer, namely the number of times, and sense, the image of the torus wrap around the unit sphere, characterizes each class. The skyrmion number is given by $q_s = 1/4\pi \int dx\, dy\, \hat{n} \cdot \partial_x \hat{n} \times \partial_y \hat{n}$. A close inspection of the arrow patterns in **a** reveals that before the monopole event (marked by the red dot), the skyrmion number is −1, whereas after the monopole event it is 0. An analogous figure can be drawn for an anti-monopole across which the skyrmion number jumps by −1. Haldane showed that associated with each charge q_m monopole event there is a phase factor, $\eta_{\mathcal{R}}^{q_m}$, which enters the path integral over all possible $\hat{n}$ configurations in space and (imaginary) time[5]. This phase factor depends on the spatial location of the monopole core, which it is natural to associate with the centre of a lattice plaquette, $\mathcal{R}$. There is some arbitrariness in the choice of $\eta_{\mathcal{R}}$, but a consistent pattern for spin 1/2 on a square lattice is shown in **b** and for spin 1 in **c**.

accounts for the two nematic ground states depicted in Fig. 4. If we introduce a perturbation that breaks the crystal 90° rotation symmetry, the absolute value of the Feynman amplitudes associated with monopoles sitting at the +1 and −1 locations in Fig. 2c no longer need to be the same, hence their Feynman amplitudes no longer cancel, which means the odd q_m monopoles can proliferate, rendering the PM state non-degenerate. This observation justifies identifying the two-fold degeneracy in the symmetric system with spontaneous breaking of 90° rotation symmetry.

In the following discussions we will use Euclidean spacetime and denote the imaginary time as τ. Consider a 4-component real vector field of unit norm, $\hat{\Omega}(x, y, \tau) = (\mathbf{\Omega}, \Omega_4)$ with $|\hat{\Omega}|^2 = 1$, whose first three components, $\mathbf{\Omega}(x, y, \tau)$ are the Néel order parameter and Ω_4 is the Ising-like nematic order parameter. For example, for a spin model on a square lattice, we can take $\Omega_4(x_i, y_i, \tau) \propto \langle \mathbf{S}_i \cdot \mathbf{S}_{i+\hat{x}} - \mathbf{S}_i \cdot \mathbf{S}_{i+\hat{y}} \rangle$. The nonlinear sigma model action we shall consider is

$$S = \int d^2x\, d\tau \left[\frac{1}{2g} |\partial_\mu \hat{\Omega}|^2 + V(\Omega_4^2) \right] + i\frac{\Theta}{2\pi^2} \int d^2x\, d\tau\, \epsilon^{abcd} \Omega_a \partial_x \Omega_b \partial_y \Omega_c \partial_\tau \Omega_d \qquad (3)$$

where $\Theta = \pi$ and ϵ is the Levi-Civita symbol. This field theory has been introduced in refs 26,27, which discuss the effects of topological terms on the spectrum and phases of nonlinear sigma models. For our purposes a derivation of equation (3) is given in the Supplementary Information. Note that this particular topological term is possible only in spatial dimension $d = 2$ with a $N = 4$ component order parameter. Here V is an anisotropy term that favours the first three components of $\hat{\Omega}$, (for example $V = \Delta[\Omega_4]^2$), hence equation (3) has $O(3) \times Z_2$ symmetry. Consider a monopole configuration centred on the origin, $(x, y, \tau) = (0, 0, 0)$. Because of the anisotropy term, $\hat{\Omega}$ on a two-sphere (S^2) in spacetime far away from the centre of the monopole is largely constrained to lie in the space spanned by the first three components of $\hat{\Omega}$—that is, $\hat{\Omega} \approx (\hat{n}, 0)$. Topologically the configurations of $\hat{n}$ on the two-sphere are classified by the skyrmion number which, in this case, is equal to the monopole charge q_m. However, such far-field configuration can be compatible with two different Ω_4 orientations in the monopole core. Consider the following configurations which reduce to the same $q_m = 1$ configuration in $\hat{n}$ far from the monopole centre

$$\hat{\Omega}^{(\pm)}(x, y, \rho) = \left(\sin\phi_\pm(\rho)\hat{n}(x, y, \rho), \cos\phi_\pm(\rho) \right) \qquad (4)$$

In equation (4) $\rho = \sqrt{x^2 + y^2 + \tau^2}/R$, $\phi_+(\rho) = \pi/2 \tanh(\rho)$ and $\phi_-(\rho) = \pi(1 - 1/2 \tanh(\rho))$. Here R is the size of the 'monopole core'. $\hat{\Omega}^{(\pm)}$ both describe $q_m = 1$ monopoles but with $\hat{\Omega} = (0, \pm 1)$ in the monopole core. It is straightforward to show that $\exp\{i\Theta/2\pi^2 \int d^2x\, d\tau\, \epsilon^{abcd} \Omega_a \partial_x \Omega_b \partial_y \Omega_c \partial_\tau \Omega_d\} = e^{\pm i\pi/2} = \pm i$ for these two types of monopole. A similar discussion holds for the $q_m = -1$ monopole. It is easy to generalize the above argument to $q_m = 2$ monopoles and obtain the corresponding phase factors $e^{\pm i\pi} = -1$. A consequence of the Z_2 (nematic) symmetry is that the Feynman amplitudes of the two monopoles described above have the same absolute values.

These monopoles represent events (as a function of imaginary time) at which the skyrmion number changes. We can thus think of the quantum disordered phase as an interacting fluid of skyrmions and anti-skyrmions. Because of the destructive interference between the two types of $q_m = 1$ monopoles discussed above, events in which the skyrmion number changes by one are forbidden—the net skyrmion number is thus conserved modulo 2 and the Hilbert space breaks into an even and an odd sector. As the stiffness constant $1/g$ renormalizes to zero in the quantum disordered state, and as there is a non-zero (possibly small) density of skyrmions and anti-skyrmions, the ground-state energy in these two sectors should be equal in the thermodynamic limit. This is the ground-state degeneracy associated with the breaking of C_4 symmetry to C_2. In the Supplementary Information we discuss the effects of an explicit $C_4 \to C_2$ symmetry-breaking field.

One can also arrive at the PM phase in Fig. 3c from the stripe-ordered side by proliferating the monopole of the stripe order parameter. Generalizing the calculation of ref. 5 we find the Berry's phase factor associated with the stripe monopole is trivial. Consequently, the charge ±1 monopole can proliferate, rendering the resulting quantum disordered state non-degenerate. Here, because the symmetries of the two phases have subgroup relationship, a continuous transition is allowed in the Landau theory. We expect such a transition to be in the O(3) universality class.

Our key theoretical conclusion is that for a spin-1 model on a square lattice, any 'intermediate' quantum disordered phase

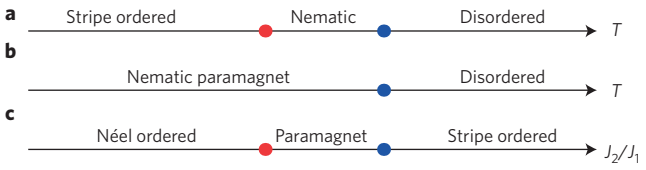

Figure 3 | Schematic phase diagrams. a, The thermal phase diagram of many iron-based superconducting materials. The blue and red dots represent two distinct phase transitions: as a function of decreasing T, the discrete crystal rotation symmetry is spontaneously broken at the blue point and continuous spin rotation symmetry at the red point. **b**, A proposed thermal phase diagram of FeSe. **c**, Zero-temperature phase diagram of the spin-1 J_1–J_2 model in equation (1) as a function of J_2/J_1.

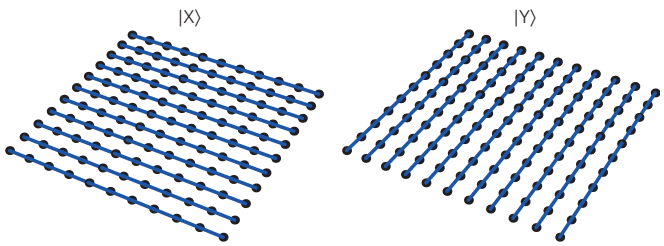

Figure 4 | The nematic paramagnetic ground states of H_K from equation (2). The solid blue lines connect AKLT-entangled pairs discussed in the main text.

between the Néel and stripe-ordered magnetic phases is likely to be a nematic PM. This is consistent with the numerical evidence for the J_1–J_2 model (equation (1)). Because the nematic quantum PM phase straddles closely between the Néel and nematic phases, we expect it to have low-lying spin excitations near both momenta $(\pi, 0)$ and (π, π). The nematic order considered here might be thought of as 'vestigial' order[28] left behind when quantum fluctuations have restored spin-rotational symmetry.

Before speculating on the relevance of these results to the interesting case of FeSe, it is necessary to comment on the effects of itinerant carriers. Angle-resolved photoemission spectroscopy (ARPES) and scanning tunnelling microscope experiments show very small electron and hole pockets for FeSe (refs 13,14,29) and at the same time quantum oscillations associated with these tiny pockets are seen[13,30]. Because the latter experiment has a very stringent requirement on the long lifetime of the quasiparticles we take it as an indication that the coupling between the itinerant carriers and the local moments is weak. This phase with decoupled magnetic and itinerant carrier degrees of freedom is analogous to the antiferromagnetic metal phase in heavy fermion systems. However, owing to the itinerant carriers the nematic phase can no longer be characterized as having a spin-gap and, close enough to criticality, the universality class of the quantum critical point is likely to be altered. In addition, FeSe is at best 'quasi-2D,' which is to say that it is ultimately three-dimensional, and this, too, will alter the nature of the phase transitions, but not necessarily affect the sequence of ordered phases.

As the iron-based superconductors involve multiple 3*d* orbitals it has been long suspected that orbital ordering is the cause of nematicity. Although we focus on the nematicity caused by frustrated magnetism, we do not intend to imply that orbital degrees of freedom play no role at all. As is well known, regardless of the driving mechanism the nematic order parameter induces orbital splitting and lattice distortion. Therefore, a cooperative effect involving many different degrees of freedom could well be necessary to describe the system behaviour quantitatively. In addition, the so-far ignored spin orbit coupling is ultimately necessary for the nematicity in the magnetic degrees of freedom to induce the band splitting observed by ARPES, the anisotropic magnetic susceptibility observed by NMR and so on.

With these caveats, the present results suggest that it may be possible to view the nematic phase in the FeSe as being driven primarily by frustrated magnetism. The fact that the underlying nematic quantum PM is gapped implies that there need not be any enhancement of the low-energy magnetic fluctuations associated with the proximity of stripe long-range order of the sort that has been detected by NMR in other Fe-based materials. Recent neutron scattering experiments[31] show relatively short-range magnetic correlations, but with reasonably large intensity (that is, with substantial magnitudes of the fluctuating moments) at the stripe ordering wavevector at low energies. Consequently, the lack of any strong evidence of slow magnetic fluctuations in NMR (ref. 20) and the short range of the magnetic correlations seen in neutron scattering seem to be entirely consistent with a magnetic origin of nematicity. As discussed previously, we expect the nematic PM phase to also exhibit spin excitations with relatively low energy at the Néel ordering wavevector. The nematic quantum PM state consists of a stacking of spontaneously formed spin-1 AF chains. It can be viewed as a 'weak' symmetry-protected topological state. A potentially testable consequence of this observation is that gapless spin-1/2 excitations can arise on certain surfaces and domain boundaries. In addition we expect nonmagnetic impurities to cut the chain and induce low-lying spin excitations in the PM gap. This can be detected by electron spin resonance in a manner analogous to that done for spin-1 chains[32]. Further experimental studies of nematic order and fluctuations in these materials—including elastoresistance, nuclear quadrupole resonance, and Raman scattering studies—as well more complete neutron scattering studies of the magnetic fluctuations would clearly be helpful.

Finally after the submission of our paper, related theoretical studies appeared[33,34], including one based on an itinerant electron picture of the nematicity in FeSe (ref. 35).

Received 29 January 2015; accepted 31 July 2015;
published online 7 September 2015

References

1. Anderson, P. W. The resonating valence bond state in La_2CuO_4 and superconductivity. *Science* **235,** 1196–1198 (1987).
2. Figueirido, F. *et al.* Exact diagonalization of finite frustrated spin-1/2 Heisenberg models. *Phys. Rev. B* **41,** 4619–4632 (1990).
3. Jiang, H.-C., Yao, H. & Balents, L. Spin liquid ground state of the spin-1/2 square J_1–J_2 Heisenberg model. *Phys. Rev. B* **86,** 024424 (2012).
4. Gong, S.-S., Zhu, W., Sheng, D. N., Motrunich, O. I. & Fisher, M. P. A. Plaquette ordered phase and quantum phase diagram in the spin-1/2 J_1–J_2 square Heisenberg model. *Phys. Rev. Lett.* **113,** 027201 (2014).
5. Haldane, F. D. M. O(3) nonlinear σ model and the topological distinction between integer- and half-integer-spin antiferromagnets in two dimensions. *Phys. Rev. Lett.* **61,** 1029–1032 (1988).
6. Read, N. & Sachdev, S. Valence-bond and spin-Peierls ground states of low-dimensional quantum antiferromagnets. *Phys. Rev. Lett.* **62,** 1694–1697 (1989).
7. Qazilbash, M. M. *et al.* Electronic correlations in the iron pnictides. *Nature Phys.* **5,** 674–650 (2009).
8. Si, Q., Abrahams, E., Dai, J. & Zhu, J.-X. Correlation effects in the iron pnictides. *New J. Phys.* **11,** 045001 (2009).
9. Yin, Z. P., Haule, K. & Kotliar, G. Kinetic frustration and the nature of the magnetic and paramagnetic states in iron pnictides and iron chalcogenides. *Nature Mater.* **10,** 932–935 (2011).
10. Gretarsson, H. *et al.* Revealing the dual nature of magnetism in iron pnictides and iron chalcogenides using x-ray emission spectroscopy. *Phys. Rev. B* **84,** 100509 (2011).
11. Maletz, J. *et al.* Unusual band renormalization in the simplest iron-based superconductor $FeSe_{1-x}$. *Phys. Rev. B* **89,** 220506 (2014).
12. Nakayama, K. *et al.* Reconstruction of band structure induced by electronic nematicity in an FeSe superconductor. *Phys. Rev. Lett.* **113,** 237001 (2014).
13. Watson, M. D. *et al.* Emergence of the nematic electronic state in FeSe. *Phys. Rev. B* **91,** 155106 (2015).

14. Zhang, P. *et al.* Observation of two distinct d_{xz}/d_{yz} band splittings in FeSe. *Phys. Rev. B* **91,** 214503 (2015).
15. Chu, J.-H., Kuo, H.-H., Analytis, J. G. & Fisher, I. R. Divergent nematic susceptibility in an iron arsenide superconductor. *Science* **337,** 710–712 (2012).
16. Chandra, P., Coleman, P. & Larkin, A. Ising transition in frustrated Heisenberg models. *Phys. Rev. Lett.* **64,** 88–91 (1990).
17. Fang, C., Yao, H., Tsai, W.-F., Hu, J. & Kivelson, S. A. Theory of electron nematic order in LaFeAsO. *Phys. Rev. B* **77,** 224509 (2008).
18. Xu, C., Müller, M. & Sachdev, S. Ising and spin orders in the iron-based superconductors. *Phys. Rev. B* **78,** 020501 (2008).
19. Baek, S.-H. *et al.* Orbital-driven nematicity in FeSe. *Nature Mater.* **14,** 210–214 (2015).
20. Böhmer, A. E. *et al.* Origin of the tetragonal-to-orthorhombic (nematic) phase transition in FeSe: A combined thermodynamic and NMR study. *Phys. Rev. Lett.* **114,** 027001 (2015).
21. Affleck, I., Kennedy, T., Lieb, E. H. & Tasaki, H. Rigorous results on valence-bond ground states in antiferromagnets. *Phys. Rev. Lett.* **59,** 799–802 (1987).
22. Arovas, D. P., Auerbach, A. & Haldane, F. D. M. Extended Heisenberg models of antiferromagnetism: Analogies to the fractional quantum Hall effect. *Phys. Rev. Lett.* **60,** 531–534 (1988).
23. Peschel, I. & Emery, V. Calculation of spin correlations in two-dimensional Ising systems from one-dimensional kinetic models. *Z. Phys. B* **43,** 241–249 (1981).
24. Jiang, H. C. *et al.* Phase diagram of the frustrated spatially-anisotropic $s=1$ antiferromagnet on a square lattice. *Phys. Rev. B* **79,** 174409 (2009).
25. Senthil, T., Vishwanath, A., Balents, L., Sachdev, S. & Fisher, M. P. A. Deconfined quantum critical points. *Science* **303,** 1490–1494 (2004).
26. Abanov, A. & Wiegmann, P. Theta-terms in nonlinear sigma-models. *Nucl. Phys. B* **570,** 685–698 (2000).
27. Xu, C. & Ludwig, A. W. W. Nonperturbative effects of a topological theta term on principal chiral nonlinear sigma models in $2+1$ dimensions. *Phys. Rev. Lett.* **110,** 200405 (2013).
28. Nie, L., Tarjus, G. & Kivelson, S. A. Quenched disorder and vestigial nematicity in the pseudogap regime of the cuprates. *Proc. Natl Acad. Sci. USA* **111,** 7980–7985 (2014).
29. Kasahara, S. *et al.* Field-induced superconducting phase of FeSe in the BCS-BEC cross-over. *Proc. Natl Acad. Sci. USA* **111,** 16309–16313 (2014).
30. Terashima, T. *et al.* Anomalous Fermi surface in FeSe seen by Shubnikov–de Haas oscillation measurements. *Phys. Rev. B* **90,** 144517 (2014).
31. Wang, Q. *et al.* Strong interplay between stripe spin fluctuations, nematicity and superconductivity in FeSe. Preprint at http://arXiv.org/pdf/1502.07544 (2015).
32. Glarum, S. H., Geschwind, S., Lee, K. M., Kaplan, M. L. & Michel, J. Observation of fractional spin $S=1/2$ on open ends of $S=1$ linear antiferromagnetic chains: Nonmagnetic doping. *Phys. Rev. Lett.* **67,** 1614–1617 (1991).
33. Glasbrenner, J. K., Mazin, I. I., Jeschke, H. O., Hirschfeld, P. J. & Valent, R. Effect of magnetic frustration on nematicity and superconductivity in Fe chalcogenides. http://dx.doi.org/10.1038/nphys3434 (2015).
34. Rong, Y. & Si, Q. Antiferroquadrupolar and Ising-nematic orders of a frustrated bilinear-biquadratic Heisenberg model and implications for the magnetism of FeSe. Preprint at http://arXiv.org/pdf/1501.05926 (2015).
35. Chubukov, A. V., Fernandes, R. M. & Schmalian, J. Origin of nematic order in FeSe. *Phys. Rev. B* **91,** 201105 (2015).

Acknowledgements

We thank H. Jiang and T. Xiang for useful discussions. F.W. was supported by the National Key Basic Research Program of China (Grant No. 2014CB920902) and the National Science Foundation of China (Grant No. 11374018). S.A.K. was supported in part by the US Department of Energy, Office of Science, Basic Energy Sciences, Materials Sciences and Engineering Division, grant DE-AC02-76SF00515 at Stanford. D.-H.L. was supported by the US Department of Energy, Office of Science, Basic Energy Sciences, Materials Sciences and Engineering Division, grant DE-AC02-05CH11231. D.-H.L. and S.A.K. would like to thank KITP for hospitality, supported in part by the National Science Foundation under Grant No. NSF PHY11-25915, where the collaboration started.

Author contributions

All authors contribute equally.

Additional information

Supplementary information is available in the online version of the paper. Reprints and permissions information is available online at www.nature.com/reprints. Correspondence and requests for materials should be addressed to D.-H.L.

Competing financial interests

The authors declare no competing financial interests.